Biochemistry and Biophysics Reports 42 (2025) 102025

Contents lists available at ScienceDirect

Biochemistry and Biophysics Reports

journal homepage: www.elsevier.com/locate/bbrep

Metabolism of sphingolipids in a rat spinal cord stenosis model

Baasanjav Uranbileg [a], Yoko Hoshino [b], Mariko Ezaka [b], Makoto Kurano [a], Kanji Uchida [b], Yutaka Yatomi [a], Nobuko Ito [b,*]

[a] Department of Clinical Laboratory Medicine, Graduate School of Medicine, The University of Tokyo, Tokyo, Japan
[b] Department of Anesthesiology and Pain Relief Center, The University of Tokyo Hospital, Tokyo, Japan

ARTICLE INFO

Keywords:
Sphingolipid
ceramide
Sphingosine 1-phosphate
Lumbar spinal canal stenosis
Neuropathic pain

ABSTRACT

Background: Lumbar spinal canal stenosis (LSCS) plays a crucial role in neurogenic claudication and neuropathic pain. Recent studies suggest that changes in sphingolipid metabolism are linked to neuropathic pain. To explore the association between sphingolipids and LSCS, we measured the levels of sphingolipids and sphingolipid-associated molecules in an animal model of cauda equina compression (CEC), a typical type of LSCS.
Methods: By placing silicon blocks within the lumbar epidural space, CEC model were constructed in which motor disfunction had already been confirmed in our previous study. Quantitative measurements of various sphingolipids were conducted using LC-MS/MS in spinal cord and cerebrospinal fluid (CSF) samples on days 1, 7, and 28 following insertion of silicon blocks. Additionally, gene expression was analyzed in spinal cord tissue.
Results: In the CEC model, there was a significant increase ceramide levels in the CSF with upregulation of ceramide synthase 1 in the spinal cord tissue samples on day 1. Further, S1P levels in the CSF increased on day 7 and in the spinal cord significantly increased on day 28, and there was an increase in mRNA expression levels of sphingosine kinases (SphK)1 on days 1,7, and 28, while SphK2 on days 7 and 28. Regarding S1P receptors, there was an increase in mRNA expression levels of S1P1 on days 1,7, and 28 and S1P3 on day1.
Conclusion: The production and activation of the sphingolipid signaling pathway could play a pivotal role in neuropathic pain related to LSCS.

1. Introduction

Low back pain and numbness in the legs are main symptoms of Lumbar spinal canal stenosis (LSCS) and these symptoms intensify while walking, leading the reduced walking distance, i.e., neurogenic claudication. Prolonged LSCS can result in permanent damage to cauda equina nerves leading to persistent neurogenic claudication and neuropathic pain [1–4]. Neuropathic pain due to LSCS become refractory to treatment with nonsteroidal and anti-inflammatory drugs and opioids. Reportedly, the incidence of LSCS is approximately 10 % in individuals aged ≥70 [2–4].

Bioactive lipids, such as sphingolipids, glycerophospholipids, and eicosanoids, have been shown to have powerful physiological effects and play a role in the development of disease conditions. Recent technological advances in mass spectrometry and chromatography have enabled the analysis of diverse lipid profiles and applied to elucidate the mechanism of disease progression and search the novel biomarkers through the analysis of reproducible animal models and human cohorts [5–11]. In our previous studies, we developed a cauda equina compression (CEC) model, which stimulated the main cause of LSCS along with motor dysfunction and intermittent claudication and measure lysophosphatidic acid (LPA) and its precursor lysophosphatidylcholine (LPC) using liquid chromatography-mass spectrometry (LC-MS/MS). LPA have been known as a potent bioactive lipids involved in neuropathic pain initiation and maintenance [12]. In these studies, we observed significantly increased LPC and LPA levels in the cerebrospinal fluid (CSF) from day 1, which was consistent with CSF data from patients with LSCS [13]. We also explored the importance of the LPC/autotaxin/LPA axis as one of the main mechanisms in neuropathic pain using a rat model of LSCS [14,15].

In addition to LPA, other bioactive lipids, sphingosine 1-phosphate (S1P) and ceramide, reported to play versatile roles in cellular responses. S1P is a sphingolipid involved in regulating various cellular responses such as growth, proliferation, migration, survival, and inflammation through the recruitment of immune cells. When secreted

* Corresponding author. Department of Anesthesiology and Pain Relief Center, Graduate School of Medicine, The University of Tokyo, 7Hongo, Bunkyo-ku, Tokyo, 113-8655, Japan.
E-mail address: nobuko-tky@g.ecc.u-tokyo.ac.jp (N. Ito).

https://doi.org/10.1016/j.bbrep.2025.102025
Received 25 November 2024; Received in revised form 7 April 2025; Accepted 18 April 2025

List of abbreviations

CEC	Cauda equina compression
CERS	Ceramide synthase
CSF	cerebrospinal fluid
LC-MS/MS	Liquid chromatography tandem-mass spectrometry
LPA	lysophosphatidic acid
LPC	lysophosphatidylcholine;
LSCS	lumbar spinal canal stenosis
S1P	sphingosine 1-phosphate
dhS1P	dihydrosphingosine 1-phosphate
dhSph	dihydrosphingosine
SMase	sphingomyelinase
SphKs	sphingosine kinases
SPT	serine palmitoyl transferase

to the extracellular milieu, S1P acts as an extracellular messenger by the activation of five specific G protein-coupled receptors (S1P1–S1P5) [16–18]. S1P is produced from sphingosine phosphorylation by sphingosine kinases (SphK) 1 and 2, which are found in most tissues, while its precursor sphingosine is produced from ceramide by a ceramidase. Ceramide plays a role in various cellular responses involved in cell cycle arrest and apoptotic cell death, being a central hub in sphingolipid metabolism. There are three pathways of ceramide synthesis: the de novo pathway, the sphingomyelinase (SMase) pathway, and the salvage pathway [19–21]. The de novo pathway is initiated in the endoplasmic reticulum by the action of serine palmitoyl transferase (SPT) using serine and Palmitoyl-CoA as a substrate, following the production of dihydrosphingosine (dhSph) as an intermediate. Then N-acylation of dhSph is carried out by ceramide synthase (CERS), yielding dihydroceramide and ceramide is synthesized by the action of desaturases. SMase are enzymes responsible for generating ceramide and Phosphocholine by hydrolyzing sphingomyelin at the plasma membrane. In the salvage pathway, sphingosine produced by sphingolipid metabolism is converted to ceramide by the action of CERS again and reused. The SMase and salvage pathways are responsible for supplying ceramide, enabling prompt cellular signaling in response to various stimuli [22,23]. Finally, the ceramide produced by these pathways is rapidly metabolized and converted to sphingosine and S1P (Fig. 1).

Emerging evidence indicates that S1P and ceramide share potent inflammatory and nociceptive effects [24–26]. Both S1P and ceramide were reported to induce hyperalgesia when provided through intradermal injection [27,28], and their levels increased in the spinal cord of a rodent model of peripheral nerve injury, indicating that both are potential treatment targets for neuropathic pain [29–31]. To induce neuropathic pain, these studies used direct approach to the nerves, such as peripheral nerve ligation and chemical-induced peripheral nerve responses. However, it remains unclear whether S1P or ceramide was involved in the LSCS model, which spinal cord were compressed from epidural space. In our study, we used an LSCS model similar to human CEC, which indirectly compresses the spinal cord and induces the

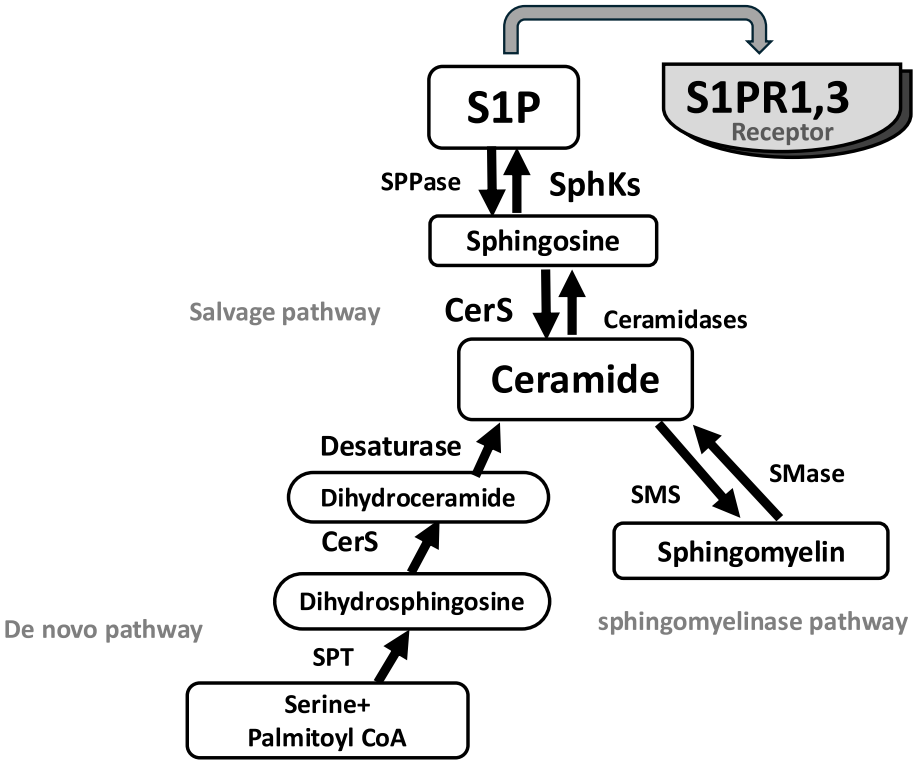

Fig. 1. S1P and Ceramide synthesis and metabolic pathway
Ceramide is central hub of sphingolipid metabolism. There is three ways to produce ceramide, one from sphingomyelin (SM) by the action of the sphingomyelinases (SMase), one is the de novo biosynthesis by the action of the serine palmitoyl transferase (SPT) using serine and Palmitoyl-CoA as a substrate, following the production of dihydrosphingosine (dhSph) as an intermediate.dhSph is acylated by the action of ceramide synthase (CERS) to produce dihydroceramide and finally, ceramide is synthesized by the action of desaturase. Another one is salvage pathway by which recycling of free sphingosine produced from the degradation of preformed sphingolipids by the action of CERS. Sphingosine is phosphorylated by the enzyme SphKs to produce S1P. S1P plays a various cellular function through its five specific G-protein coupled receptors, i.e. S1P1 and S1P3. Of the S1P receptors, S1P1, S1P2 and S1P3 are expressed in sensory neurons, where S1P1 and S1P3 have been reported to play important roles in regulating nociceptor function. S1P1 and S1P3 are also expressed in both microglia and astrocytes. S1P: sphingosine 1-phosphate, SPPase: sphingosine phosphate phosphatase, SphKs: sphingosine kinases, CerS: ceramide synthase, SMS: SMase: sphingomyelinase SPT: serine palmitoyl transferase.

reduced walking distance, i.e., neurogenic claudication.

To investigate the involvement of S1P and ceramide in LSCS, we analyzed the sphingolipid profiles of the spinal cord tissue and CSF using advanced lipidomics accompanied with LC-MS/MS and measured the expression of S1P receptors and sphingolipid-producing enzymes by qPCR in the spinal cord in the CEC model.

2. Methods

2.1. Animals

Adult female Sprague–Dawley rats (8–10 weeks old, 200–250 g) obtained from Japan SLC (Shizuoka, Japan) was used in this study. Rats were maintained in a 12 h light/12 h dark cycle with free access to food and water. Animal experiments were performed in compliance with the guidelines for the Care and Use of Laboratory Animals and were approved by the Ethics Committee for Animal Experiment of the University of Tokyo (approval No. P15-100).

2.2. Surgical procedure

The CEC model was created after anesthesia with intraperitoneal pentobarbital injection (Kyoritsu Seiyaku, Tokyo, Japan) and isoflurane inhalation (Abbott, Illinois, USA). Animals were placed in the prone position and midline incision was made using a Leica M80 stereomicroscope (Leica Microsystems, Buffalo Grove, IL, USA). After separation of the paraspinal muscles from the spinous processes at L3 to L5, two silicon blocks (King Works CO., Ltd., Osaka, Japan) were put in the epidural space at L3 and L5 levels. Following the suturing the incision, the rats were kept on a 37 °C heating mat for 1 h and returned to their cage. Samples were harvested from naïve, days 1,7, and 28 following surgeries. In this model, motor disfunction, a typical symptom of LSCS, was previously confirmed through rotarod behavior tests following a surgery [14]. Since there were no significant differences in lipids levels between the naïve control and sham groups in the previous study, the present analysis was limited to the naïve control group and CEC group [14].

2.3. Quantitative real-time polymerase chain reaction

Total RNA was extracted from spinal cord tissues of CEC models or naïve control using the GenElute mammalian total RNA minipump kit (Sigma Aldrich, St Louis County, Missouri, USA). Extracted total RNA was reverse transcribed using a Superscript^{s} First-Strand Synthesis System for RT-PCR (Roche Molecular Diagnostics, CA, USA). TaqMan qPCR was performed with TaqMan universal master mix using ABI7300 Real-Time PCR Instrument (Applied Biosystems) via the 2-ΔΔCt method. SphK1, SphK2, S1P1, S1P3, CERS, CERS2, and internal control 18s ribosomal primers and probes (TaqMan Gene Expression Assays) were obtained from Applied Biosystems (Rn00682794_g1, Rn01457923_g1, Rn02758712_s1, Rn02758880_s1, Rn01408085_s1, Rn00572952_s1, Rn01420078_m1, Rn01762797_g1 and HS99999901_s1). The samples were incubated for 10 min at 95 °C, followed by 40 cycles at 95 °C for 15 s and 60 °C for 1 min. The target gene expression level was presented as a relative expression level to ribosomal 18s mRNA.

2.4. CSF collection for sphingolipid measurements

The CSF was obtained from the cisterna magna under a Leica M80 stereomicroscopy (Leica Microsystems, Buffalo Grove, IL, USA), following a previously described method [14,15] with slight modifications. The animals were positioned prone on a stereotaxic device (David Kopf instrument, Tujunga, California, USA) under the inhaled isoflurane anesthesia. Superficial muscles were separated with bipolar forceps and underlying muscle layers were meticulously separated to confirm the dura exposure. CSF was obtained using 30G 1/2 needles (Dentronics, Tokyo, Japan) attached to a 1-mL syringe. The acquired samples (50–120 μL) were labeled and stored at −80 °C.

2.5. Measurement of sphingolipids and ceramides

Sphingolipids and ceramides were quantified using a previously described method with slight modification [32]. Homogenized spinal cord samples or CSF samples in PBS were mixed with 0.1 % formic acid in methanol (Wako Pure Chemical Industries, Japan) containing internal standards. For the internal standards, C17 S1P, C17 dihydro S1P, C17:1 Sphingosine (Sph), C17:1 dihydrosphingosine (dhSph) and d18:1/17:0 Ceramide (Avanti Polar Lipids, Alabama) at 1.0 ng/mL (final concentration) were added. After sonication, the samples were centrifuged at 12,000 g for 10 min at 4 °C.The collected supernatants were subjected for LC-MS/MS analysis.

The LC-MS/MS analysis with multiple-reaction monitoring (MRM) was conducted using HPLC and LC-8060 combined with quantum triple-quadrupole mass spectrometer (SHIMADZU, Japan). Seven ceramide species (Cer d18:1/16:0, Cer d18:1/18:0, Cer d18:1/18:1, Cer d18:1/20:0, Cer d18:1/22:0, Cer d18:1/24:0, Cer d18:1/24:1), dhSph, dhS1P, Sph and S1P were measured. Samples were separated on an InertSustain Swift C8 PEEK column (3 μm 150 × 2.1 mm, GL Science, Japan) with a gradient elution of solvent A (MilliQ water/0.3 % formic acid) and solvent B (acetonitrile/0.3 % formic acid) at temperature 45 °C. Separation of analytes was accomplished using a 12-min binary gradient. The proportion of solvent B was 40 % at first, linearly increased to 85 % over 1 min, held at 85 % for 1–3 min, increased to 95 % for 3–5 min, and re-equilibrated at 40 % for 5–10 min. Compounds were measured in the electrospray ionization positive ion mode under the following analytical protocol: nebulizer gas flow set at 3.0 L/min, drying gas flow set at 8.0 L/min, heating gas flow set at 8.0 L/min, interface temperature at 100 °C, desolvation temperature at 150 °C, and heat block temperature at 250 °C. The data were analyzed using the Lab Solution software (SHIMADZU), with standard curves employed to calculate the area ratio (peak area of analyte/peak area of internal standard).

2.6. Statistical analysis

Data processing and analysis were performed using R statistical software version 3.3.1 (http://www.r-project.org) and GraphPad Prism 8.0 software (GraphPad Software, San Diego, CA).

A paired *t*-test, one-way ANOVA, and mixed-effect analysis were used to analyze differences in mRNA levels of all measured markers and sphingolipids levels in CSF. The sphingolipids results are expressed as means and standard deviations. A P-value <0.05 was considered to indicate statistical significance.

3. Results

3.1. In the CEC model, S1P levels increased in the compressed part of the spinal cord

At each time point, sphingolipid concentrations were measured in the spinal cord tissue samples collected from the area compressed by the silicon block (Fig. 2A and B n = 4–6). The S1P level was significantly higher at day 28 than in the naïve group, and the sphingosine level increased transiently (Fig. 2A). Conversely, there were no significant differences in the levels of dhSph and dihydrosphingosine 1-phosphate (dhS1P) in the spinal cord samples (Fig. 2A). Among the detected ceramide species, ceramide 24:1 was most abundant species in the epicenter spinal cord tissues. The level of Ceramide 24:1 tend to increase at day1 and significantly decreased at day7 and day 28 compared with the day1 group (Fig. 2 B).

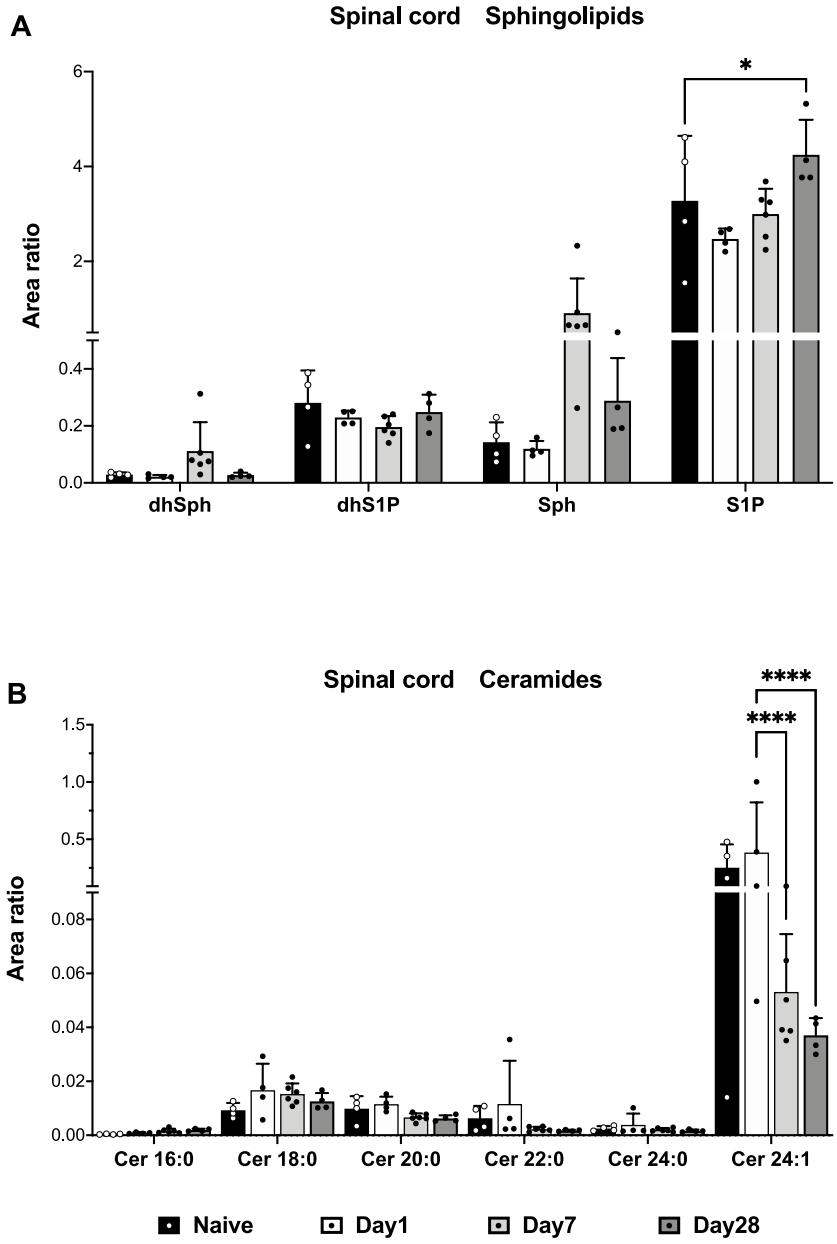

Fig. 2. Quantitative analysis of changes in sphingolipid and ceramide levels over time in the spinal cord tissue subjected to spinal cord compression. Quantitative measurements of A) four sphingolipids (dhSph, dhS1P, Sph, and S1P) and B) six ceramides (Cer16:0, Cer18:0, Cer20:0, Cer22:0, Cer24:0, and Cer24:1) in the spinal cord of naïve rats and rats subjected to silicone compression for 1, 7, and 28 days. n = 4–6. A significant increase in S1P was observed on day 28 compared with the naïve controls. Conversely, the Cer24:1 level tends to increase on day1 and significantly decreased on days 7 and 28 compared to day 1. Statistical analyses were conducted using two-way ANOVA followed by Tukey's multiple comparison test. P < 0.05*, <0.0001****.

3.2. In the CEC model, S1P, ceramide 22:0, and ceramide 24:1 level was elevated in the CSF

Sphingolipids were measured in CSF samples obtained at a similar sampling time as the tissue samples (Fig. 3A and B n = 3–8). The S1P level gradually increased after surgery and reached a significantly high level at day 7 compared with the naïve group, returning to the same level as the naïve group by day 28 (Fig. 3A). The sphingosine level was significantly low throughout the study period in the CEC model (Fig. 3A), suggesting that sphingosine was consumed for S1P production. The ceramide 24:1 level increased 20-fold compared with the naïve group, with significant increases on days 1 and 7 compared to the naïve group. Similarly, ceramide 22:0 levels increased in CSF samples of CEC models throughout the study period, being significantly higher at day 1 compared with the naïve group (Fig. 3B). There were no significant differences in dhSph and dhS1P levels in CSF samples (Fig. 3A).

3.3. In the CEC model, there was increased SphKs and CERS expression

We further studied the sphingolipid metabolic pathway to investigate the underlying enzymes contributing to the observed increase in S1P and ceramide levels (Fig. 1). Since motor dysfunction was induced by spinal cord compression, we exclusively used spinal cord tissue samples from the CEC model. First, we measured expression levels of SphK1 and SphK2 at days 1, 7, and 28 after the surgery and compared them to the naïve group (Fig. 4A and B n = 3–6). SphK1 expression in the

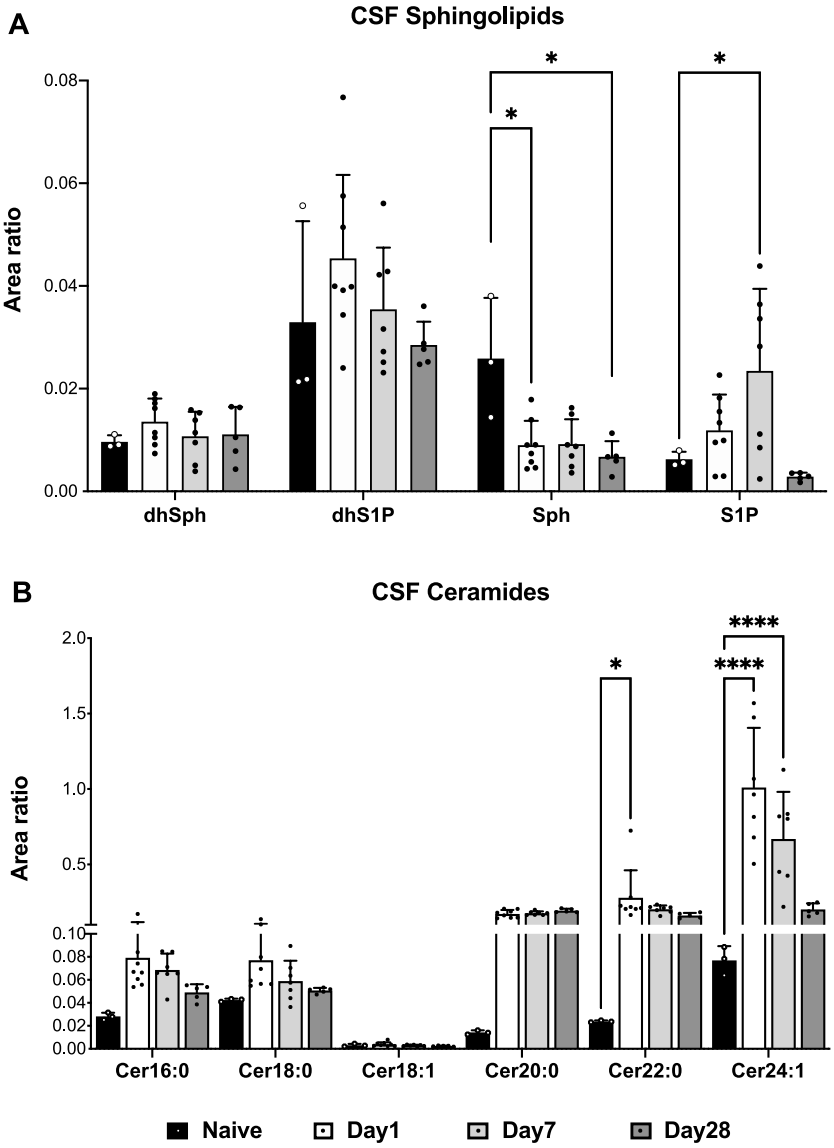

Fig. 3. Quantitative analysis of changes in sphingolipid and ceramide levels in cerebrospinal fluid (CSF) subjected to spinal cord compression over time. Quantitative measurements of A) four sphingolipids (dhSph, dhS1P, Sph, and S1P) and B) six ceramides (Cer16:0, Cer18:0, Cer18:1, Cer20:0, Cer22:0, and Cer24:1) in the CSF of naïve rats and rats subjected to spinal cord compression for 1, 7, and 28 days. A significant decrease in Sph was observed on days 1 and 28 compared to the naïve controls. S1P also increased significantly after 7 days. Cer22:0 levels increased on day1, and the Cer24:1 level significantly increased on days 1 and 7 compared to naïve. n = 3–8. Statistical analyses were conducted using two-way ANOVA followed by Tukey's multiple comparison test. P < 0.05*, <0.0001****.

CEC model increased significantly from day 1 and remained consistently high until day 28 (Fig. 4A). Similarly, SphK2 expression gradually increased, with significant changes detected from day 7 (Fig. 4B).

Based on the significant increase in the ceramide level, we measured the levels of CERS as described in Figure 1. CERS has six family members that differ based on the synthesized ceramide acyl chain lengths. Of these, CERS1 is commonly and CERS2 is moderately expressed in neuronal system [33]. Based on this, we measured CERS1 and CERS2 expression in the CEC model's tissues (Fig. 4C and D n = 4–10). CERS1 expression significantly increased on days 1 and 28; however, CERS2 expression remained unchanged. It was expected that ceramide synthesis, especially through CERS1, increased following the spinal cord compression.

3.4. S1PR1 and S1PR3 upregulation in the spinal cord in the CEC model

S1P released to the extracellular milieu initiates signaling through a family of five cognate G protein-coupled receptors (S1PR1-5) facilitating various cellular responses [34,35]. We next measured S1P1 and S1P3 expression in the spinal cord of the CEC model. S1P1 and S1P3 are the predominant subtypes in astrocytes and microglia, and their levels increase following glial cell activation [36]. We found that S1P1 and S1P3 levels increased in the epicenter spinal cord tissue (Fig. 5A and B n = 3–6).

It was suggested that S1P could act through its receptors S1P1 and S1P3 and enhance the activation of microglia and astrocytes following spinal cord compression.

4. Discussion

In this study, we analyzed sphingolipid profile of spinal cord tissue and CSF by using advanced lipidomics combined with LC-MS/MS and mRNA expression levels of sphingolipid-related factors in the CEC model. There was a significant increase ceramide levels in the CSF with

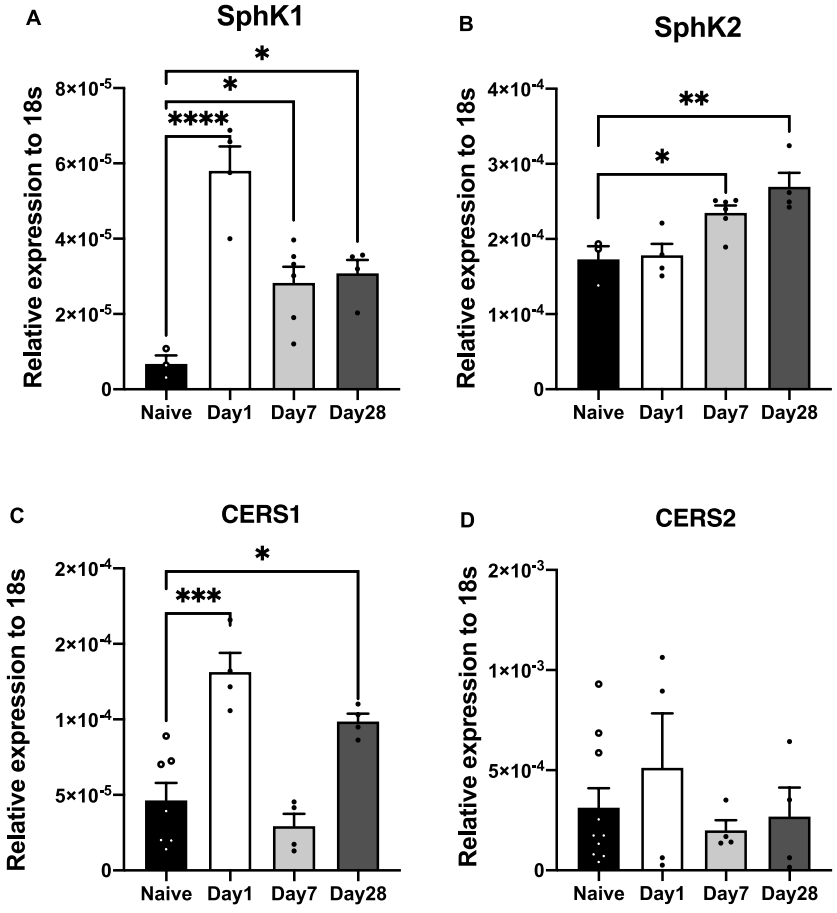

Fig. 4. mRNA expression of various sphingosine kinases (SphKs) and ceramide synthase (CERS) in the spinal cord after spinal cord compression. Quantitative PCR analysis revealed A) a significant increase in SphK1 mRNA expression throughout the experimental period (days 1, 7, and 28). B) significant upregulation of SphK2 mRNA expression at days 7 and 28, C) and of CERS1 mRNA expression at 1- and 28-days post-suegery. Conversely, D) CERS2 mRNA levels did not differ from the controls. A) B) n = 3–6. C)D) n = 4–10. Statistical analyses were conducted using one-way ANOVA followed by Tukey's multiple comparison test. P < 0.05*, <0.01**, <0.001***, <0.0001****.

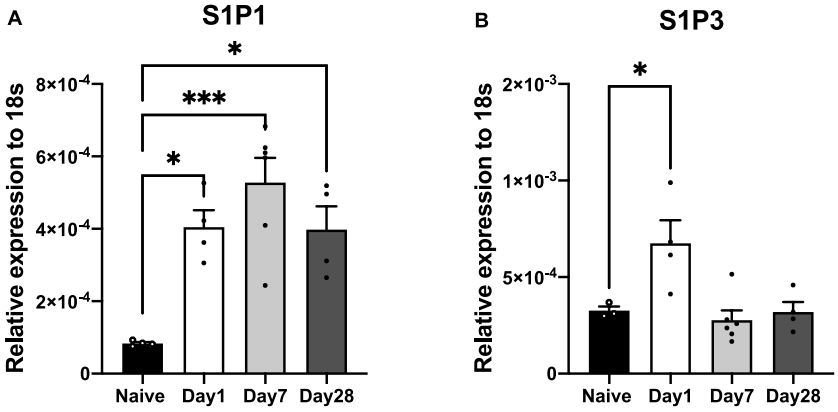

Fig. 5. mRNA expression of the G-protein-coupled receptor for S1P (S1P1, S1P3) in the spinal cord after spinal cord compression. Quantitative PCR analysis revealed A) a significant increase in S1P1 mRNA expression throughout the experimental period (days 1, 7, and 28) and B) significant upregulation of S1P3 mRNA expression at day 1. n = 3–6. Statistical analyses were conducted using one-way ANOVA followed by Tukey's multiple comparison test. P < 0.05*, <0.001***.

upregulation of CERS1 in the spinal cord tissue samples on day 1. Additionally, S1P levels in the CSF significantly increased on day 7, and there was upregulation of SphK1 on days 1,7, and 28, while SphK2 on days 7 and 28. Regarding S1P receptors, there was an increase in mRNA expression levels of S1P1 on days 1,7, and 28 and S1P3 on day1. These results suggest that ceramide and S1P produced in the spinal cord tissues were potently involved in the mechanism of LSCS.

S1P has been shown to play a potent role in neuropathic pain through

its specific receptors, especially S1P1. S1P and S1P1 signaling has been involved in the regulation of pain pathways, its dysregulation can contribute to the development and maintenance of neuropathic pain [37,38]. Chen et al. reported that the S1P level in the spinal cord increased after nerve injury and during neuropathic pain attenuation by S1P1 antagonists, revealing that S1P–S1P1 signaling has an important role in neuropathic pain [30]. Similarly, our findings showed increased S1P levels in the CSF and epicenter of the spinal cord tissue samples along with consistently increased S1P1 expression in the spinal cord tissue samples of the CEC model (Figs. 2A, 3A and 5A). In addition to S1P1, S1P3 expression increased in this model, suggesting the involvement of S1P–S1P3 signaling in neuropathic pain. S1P1 and S1P3 are the most abundant receptor subtypes expressed in microglia and astrocytes, and their expression increases in response to glial activation, resulting in the release of interleukin-1 β and enhancing the neuroinflammatory responses [36]. In our previous work, we observed significantly increased presence of CD11b-positive microglial cells in the dorsal horn of the spinal cord in this CEC model [14]. We speculate that increased S1P production due to SphKs activation triggers signaling through S1P1 and S1P3 receptors on microglia, releasing various inflammatory cytokines and mediators from microglia and potentially driving neuroinflammation and hypersensitivity. Previously, S1P3 was shown to be highly expressed on cultured astrocytes and S1P induce inflammatory responses through S1P3 in astrocytes [39]. Despite the unclear involvement of astrocytes in this model, proof of astrocyte activation by evaluating the expression of Glial fibrillary acidic protein, one of the astrocyte markers, is expected in the future. Another study reported that S1P and its receptor, S1P1 play a role in the migration of neural stem cells toward the site of spinal cord injury and may contribute to damage repairing following spinal cord injury [40]. They confirmed that S1P concentration increased at the site of spinal cord injury in which microglia were accumulated. Additionally, S1P enhance the viability, and differentiation of neural stem cells through its receptor S1P1, indicating that S1P may be an important neuroprotective factor released from microglia. [40,41]. There are various studies, which employed the S1P1 agonist FTY720 to attenuate glial cell death and demyelination in *vitro* and *ex vivo* Multiple Sclerosis models and enhance remyelination [42–45]. Thus, S1P–S1P1 signaling not only increases the neuroinflammation through the activation of microglia but also play a potential role in repairing the damage. Detailed evaluations at each time point are needed to determine whether elevated S1P levels are linked to neuroprotective or neurotoxic effects. By evaluating when the S1P/S1P1 axis is tilting towards a balance between neuroinflammation and neuroprotection, it may provide a new therapeutic approach tailored to the progression of LSCS.

In addition to S1P, our findings strongly suggest the involvement of ceramide in LSCS as evidenced by the significant changes in ceramide levels observed in the CEC model (Figs. 2B and 3B). A significant increase in C24:1 and C22:0 ceramide levels were observed in the CSF samples. Long acyl chain ceramides comprise >80 % of the total ceramide content in the spinal cord [8]. Our results suggest that C24:1 ceramide and C22:0 ceramide, which are originally abundant in the spinal cord tissue, increased in the epicenter of the spinal cord tissue of the CEC model and leaked into the CSF. Moreover, our results of increase of CERS expression suggest acceleration of the pathway of ceramide synthesis in the spinal cord.CERS is a key enzyme to produce ceramide from dhSph or reproduce ceramide from sphingosine [21,23,46].The synthesis of the ceramide with very long acyl chains is known to be synthesized by CERS2 [46,47]. We observed an increase in CERS1 expression, which mainly uses C18-CoA, but not of CERS2, which mainly uses C24-CoA and C22-CoA in the epicenter of the spinal cord. It has been also shown that C24:1 and C22:0 Sphingomyelin account for >50 % of the sphingomyelin in the spinal cord tissue [8]. Considering that the species of sphingomyelin with very long acyl chains are contributing to an increase in ceramides with very long acyl chains, there is a possibility that C24:1 and C22:0 ceramide produced through the SMase pathway, i.e., sphingomyelin degradation, is increased in this CEC model. SMase are activated by stress stimuli and inflammatory cytokines, and degraded ceramide by SMase is rapidly metabolized to sphingosine, which is then converted to S1P [19–21,23]. The increased ceramide level through the SMase pathway might be responsible for the increase in S1P in this CEC model. We speculate that in addition to the SMase pathway, the ceramide production pathway, i.e., salvage pathway also works simultaneously to regulate the amount of ceramide in this model. To ascertain whether the SMase pathway is the major ceramide synthesis pathway in the CEC model, further studies that confirm the activation of SMase and ceramidase in the epicenter of the spinal cord and precise lipid analysis of sphingomyelin species will be needed. It was reported that intrathecal injection of the neutral-SMase inhibitor GW4869 reduces microglial activation and tactile allodynia [29]. Enzymes in the ceramide synthesis pathway could be strong targets for ameliorating the symptoms of neuropathic pain in the CEC model. Whereas another possible reason for the increase in ceramide levels in CSF might be the effect of change in sphingolipid metabolism in ependymal cells following spinal compression, and further research at the cellular level is also needed.

While ceramides with a C18 acyl chain have been related to apoptosis induction [48,49], there are few studies on the specific functions of ceramide species with different acyl chain lengths. Ceramide has also been noticed as a potential bioactive lipid involved in the development of various pain stimuli [24,26]. Intradermal injection of ceramide into rat hind paw induces hyperalgesia [28,50,51], and intrathecal injection of the CERS inhibitor attenuated the neuropathic pain induced by partial sciatic nerve ligation [29]. Ceramide activates primary microglial cells [52,53]. Ceramide and S1P cause the activation of microglia, which may contribute to subsequent inflammatory mediator release and central sensitization in the spinal cord. Moreover, ceramide has been reported to facilitate Tetrodotoxin -resistant sodium current in cultured rat sensory neurons [54]. Although most experimental studies have used ceramide with a C18 acyl chain, ceramide with a very long acyl chain has not been studied. Further studies need to focus on clarifying whether ceramides with long acyl chains are involved in neuroinflammation and the underlying mechanisms of neuropathic pain.

A noteworthy result of this study is that an increase in S1P and ceramide was observed in the CSF of a LSCS model. No change in sphingolipids was observed in the plasma (data not shown). Sphingolipids detected in the CSF may reflect the severity of the disease and the effectiveness of treatment as a potent new biomarker. To support this observation, it will be necessary to analyze CSF data from patients with LSCS in the future. Further precise lipid analysis of sphingolipids and altered expression of metabolite-producing enzymes will lead to new therapeutic strategies for LSCS.

5. Conclusion

In CEC rats, we observed increased S1P and ceramide levels in the CSF and increased SphKs, S1P1, S1P3, and CERS expression in the spinal cord tissue. Our results suggest that S1P and ceramides may play a crucial role in the pathophysiology of neuropathic pain and contribute to the development of new management strategies for CEC with neuropathic pain.

CRediT authorship contribution statement

Baasanjav Uranbileg: Writing – original draft, Formal analysis, Data curation. **Yoko Hoshino:** Formal analysis. **Mariko Ezaka:** Formal analysis. **Makoto Kurano:** Writing – review & editing. **Kanji Uchida:** Writing – review & editing. **Yutaka Yatomi:** Writing – review & editing. **Nobuko Ito:** Writing – review & editing, Writing – original draft, Formal analysis, Data curation, Conceptualization.

Availability of data and materials

The datasets used and/or analyzed during the current study are available from the corresponding author on reasonable request.

Ethical statement

The animal study protocol was approved by the Animal Care and Research Ethics Committee of the University of Tokyo, Japan, for studies involving animals.

Funding

This work was supported by the Research Project on Elucidation of Chronic Pain (22ek0610028h0001) from AMED and a Grant in Aid for Scientific Research, Japan Society for Promotion of Science (JSPS) (23K08402).

Declaration of competing interest

The authors declare that they have no known competing financial interests or personal relationships that could have appeared to influence the work reported in this paper.

Acknowledgements

We would like to thank Ms. Hasegawa (Dept. of Anesthesiology, Faculty of Medicine, The University of Tokyo) for experimental support.

References

[1] E. Siebert, H. Prüss, R. Klingebiel, V. Failli, K.M. Einhäupl, J.M. Schwab, Lumbar spinal stenosis: syndrome, diagnostics and treatment, Nat. Rev. Neurol. 5 (7) (2009) 392–403.
[2] L. Kalichman, R. Cole, D.H. Kim, L. Li, P. Suri, A. Guermazi, et al., Spinal stenosis prevalence and association with symptoms: the Framingham Study, Spine J. 9 (7) (2009) 545–550.
[3] Y. Ishimoto, N. Yoshimura, S. Muraki, H. Yamada, K. Nagata, H. Hashizume, et al., Prevalence of symptomatic lumbar spinal stenosis and its association with physical performance in a population-based cohort in Japan: the Wakayama Spine Study, Osteoarthr. Cartil. 20 (10) (2012) 1103–1108.
[4] S. Yabuki, N. Fukumori, M. Takegami, Y. Onishi, K. Otani, M. Sekiguchi, et al., Prevalence of lumbar spinal stenosis, using the diagnostic support tool, and correlated factors in Japan: a population-based study, J. Orthop. Sci. 18 (6) (2013) 893–900.
[5] E. Demicheva, V. Dordiuk, F. Polanco Espino, K. Ushenin, S. Aboushanab, V. Shevyrin, et al., Advances in mass spectrometry-based blood metabolomics profiling for non-cancer diseases: a comprehensive review, Metabolites 14 (1) (2024).
[6] B. Uranbileg, E. Sakai, M. Kubota, H. Isago, M. Sumitani, Y. Yatomi, et al., Development of an advanced liquid chromatography-tandem mass spectrometry measurement system for simultaneous sphingolipid analysis, Sci. Rep. 14 (1) (2024) 5699.
[7] Y.Y. Zhao, X.L. Cheng, R.C. Lin, F. Wei, Lipidomics applications for disease biomarker discovery in mammal models, Biomarkers Med. 9 (2) (2015) 153–168.
[8] C. Wang, J.P. Palavicini, X. Han, A lipidomics atlas of selected sphingolipids in multiple mouse nervous system regions, Int. J. Mol. Sci. 22 (21) (2021).
[9] G. Cermenati, N. Mitro, M. Audano, R.C. Melcangi, M. Crestani, E. De Fabiani, et al., Lipids in the nervous system: from biochemistry and molecular biology to patho-physiology, Biochim. Biophys. Acta 1851 (1) (2015) 51–60.
[10] M. Kurano, Y. Saito, B. Uranbileg, D. Saigusa, K. Kano, J. Aoki, et al., Modulations of bioactive lipids and their receptors in postmortem Alzheimer's disease brains, Front. Aging Neurosci. 14 (2022) 1066578.
[11] S. Sethi, E. Brietzke, Recent advances in lipidomics: analytical and clinical perspectives, Prostag. Other Lipid Mediat. 128–129 (2017) 8–16.
[12] H. Ueda, Pathogenic mechanisms of lipid mediator lysophosphatidic acid in chronic pain, Prog. Lipid Res. 81 (2021) 101079.
[13] K. Hayakawa, M. Kurano, J. Ohya, T. Oichi, K. Kano, M. Nishikawa, et al., Lysophosphatidic acids and their substrate lysophospholipids in cerebrospinal fluid as objective biomarkers for evaluating the severity of lumbar spinal stenosis, Sci. Rep. 9 (1) (2019) 9144.
[14] B. Uranbileg, N. Ito, M. Kurano, D. Saigusa, R. Saito, A. Uruno, et al., Alteration of the lysophosphatidic acid and its precursor lysophosphatidylcholine levels in spinal cord stenosis: a study using a rat cauda equina compression model, Sci. Rep. 9 (1) (2019) 16578.
[15] B. Uranbileg, N. Ito, M. Kurano, K. Kano, K. Uchida, M. Sumitani, et al., Inhibition of autotaxin activity ameliorates neuropathic pain derived from lumbar spinal canal stenosis, Sci. Rep. 11 (1) (2021) 3984.
[16] M.J. Kluk, T. Hla, Signaling of sphingosine-1-phosphate via the S1P/EDG-family of G-protein-coupled receptors, Biochim. Biophys. Acta 1582 (1–3) (2002) 72–80.
[17] Y. Takuwa, Subtype-specific differential regulation of Rho family G proteins and cell migration by the Edg family sphingosine-1-phosphate receptors, Biochim. Biophys. Acta 1582 (1–3) (2002) 112–120.
[18] T. Hla, Signaling and biological actions of sphingosine 1-phosphate, Pharmacol. Res. 47 (5) (2003) 401–407.
[19] T.D. Mullen, Y.A. Hannun, L.M. Obeid, Ceramide synthases at the centre of sphingolipid metabolism and biology, Biochem. J. 441 (3) (2012) 789–802.
[20] Y.A. Hannun, L.M. Obeid, Principles of bioactive lipid signalling: lessons from sphingolipids, Nat. Rev. Mol. Cell Biol. 9 (2) (2008) 139–150.
[21] Y.A. Hannun, L.M. Obeid, Sphingolipids and their metabolism in physiology and disease, Nat. Rev. Mol. Cell Biol. 19 (3) (2018) 175–191.
[22] D. Canals, S. Salamone, Y.A. Hannun, Visualizing bioactive ceramides, Chem. Phys. Lipids 216 (2018) 142–151.
[23] K. Kitatani, J. Idkowiak-Baldys, Y.A. Hannun, The sphingolipid salvage pathway in ceramide metabolism and signaling, Cell. Signal. 20 (6) (2008) 1010–1018.
[24] M. Langeslag, M. Kress, The ceramide-S1P pathway as a druggable target to alleviate peripheral neuropathic pain, Expert Opin. Ther. Targets 24 (9) (2020) 869–884.
[25] D. Salvemini, T. Doyle, M. Kress, G. Nicol, Therapeutic targeting of the ceramide-to-sphingosine 1-phosphate pathway in pain, Trends Pharmacol. Sci. 34 (2) (2013) 110–118.
[26] J. Wang, G. Zheng, L. Wang, L. Meng, J. Ren, L. Shang, et al., Dysregulation of sphingolipid metabolism in pain, Front. Pharmacol. 15 (2024) 1337150.
[27] M. Camprubí-Robles, N. Mair, M. Andratsch, C. Benetti, D. Beroukas, R. Rukwied, et al., Sphingosine-1-phosphate-induced nociceptor excitation and ongoing pain behavior in mice and humans is largely mediated by S1P3 receptor, J. Neurosci. 33 (6) (2013) 2582–2592.
[28] T. Doyle, Z. Chen, C. Muscoli, L.M. Obeid, D. Salvemini, Intraplantar-injected ceramide in rats induces hyperalgesia through an NF-κB- and p38 kinase-dependent cyclooxygenase 2/prostaglandin E2 pathway, FASEB J. 25 (8) (2011) 2782–2791.
[29] Y. Kobayashi, N. Kiguchi, T. Maeda, M. Ozaki, S. Kishioka, The critical role of spinal ceramide in the development of partial sciatic nerve ligation-induced neuropathic pain in mice, Biochem. Biophys. Res. Commun. 421 (2) (2012) 318–322.
[30] Z. Chen, T.M. Doyle, L. Luongo, T.M. Largent-Milnes, L.A. Giancotti, G. Kolar, et al., Sphingosine-1-phosphate receptor 1 activation in astrocytes contributes to neuropathic pain, Proc. Natl. Acad. Sci. U. S. A 116 (21) (2019) 10557–10562.
[31] K. Stockstill, T.M. Doyle, X. Yan, Z. Chen, K. Janes, J.W. Little, et al., Dysregulation of sphingolipid metabolism contributes to bortezomib-induced neuropathic pain, J. Exp. Med. 215 (5) (2018) 1301–1313.
[32] E. Sakai, M. Kurano, Y. Morita, J. Aoki, Y. Yatomi, Establishment of a measurement system for sphingolipids in the cerebrospinal fluid based on liquid chromatography-tandem mass spectrometry, and its application in the diagnosis of carcinomatous meningitis, J Appl Lab Med 5 (4) (2020) 656–670.
[33] M. Levy, A.H. Futerman, Mammalian ceramide synthases, IUBMB Life 62 (5) (2010) 347–356.
[34] A. Cartier, T. Hla, Sphingosine 1-phosphate: lipid signaling in pathology and therapy, Science 366 (6463) (2019).
[35] S. Spiegel, S. Milstien, The outs and the ins of sphingosine-1-phosphate in immunity, Nat. Rev. Immunol. 11 (6) (2011) 403–415.
[36] R. Van Doorn, J. Van Horssen, D. Verzijl, M. Witte, E. Ronken, B. Van Het Hof, et al., Sphingosine 1-phosphate receptor 1 and 3 are upregulated in multiple sclerosis lesions, Glia 58 (12) (2010) 1465–1476.
[37] S. Squillace, S. Spiegel, D. Salvemini, Targeting the sphingosine-1-phosphate Axis for developing non-narcotic pain therapeutics, Trends Pharmacol. Sci. 41 (11) (2020) 851–867.
[38] S.K. Singh, S. Spiegel, Sphingosine-1-phosphate signaling: a novel target for simultaneous adjuvant treatment of triple negative breast cancer and chemotherapy-induced neuropathic pain, Adv Biol Regul 75 (2020) 100670.
[39] S.S. Dusaban, J. Chun, H. Rosen, N.H. Purcell, J.H. Brown, Sphingosine 1-phosphate receptor 3 and RhoA signaling mediate inflammatory gene expression in astrocytes, J. Neuroinflammation 14 (1) (2017) 111.
[40] A. Kimura, T. Ohmori, R. Ohkawa, S. Madoiwa, J. Mimuro, T. Murakami, et al., Essential roles of sphingosine 1-phosphate/S1P1 receptor axis in the migration of neural stem cells toward a site of spinal cord injury, Stem Cell. 25 (1) (2007) 115–124.
[41] J. Aarum, K. Sandberg, S.L. Haeberlein, M.A. Persson, Migration and differentiation of neural precursor cells can be directed by microglia, Proc. Natl. Acad. Sci. U. S. A 100 (26) (2003) 15983–15988.
[42] K.K. Dev, F. Mullershausen, H. Mattes, R.R. Kuhn, G. Bilbe, D. Hoyer, et al., Brain sphingosine-1-phosphate receptors: implication for FTY720 in the treatment of multiple sclerosis, Pharmacol. Ther. 117 (1) (2008) 77–93.
[43] V.E. Miron, S.K. Ludwin, P.J. Darlington, A.A. Jarjour, B. Soliven, T.E. Kennedy, et al., Fingolimod (FTY720) enhances remyelination following demyelination of organotypic cerebellar slices, Am. J. Pathol. 176 (6) (2010) 2682–2694.
[44] F. Mullershausen, L.M. Craveiro, Y. Shin, M. Cortes-Cros, F. Bassilana, M. Osinde, et al., Phosphorylated FTY720 promotes astrocyte migration through sphingosine-1-phosphate receptors, J. Neurochem. 102 (4) (2007) 1151–1161.

[45] S.A. O'Sullivan, C. O'Sullivan, L.M. Healy, K.K. Dev, G.K. Sheridan, Sphingosine 1-phosphate receptors regulate TLR4-induced CXCL5 release from astrocytes and microglia, J. Neurochem. 144 (6) (2018) 736–747.
[46] E.L. Laviad, L. Albee, I. Pankova-Kholmyansky, S. Epstein, H. Park, A.H. Merrill, et al., Characterization of ceramide synthase 2: tissue distribution, substrate specificity, and inhibition by sphingosine 1-phosphate, J. Biol. Chem. 283 (9) (2008) 5677–5684.
[47] I. Becker, L. Wang-Eckhardt, A. Yaghootfam, V. Gieselmann, M. Eckhardt, Differential expression of (dihydro)ceramide synthases in mouse brain: oligodendrocyte-specific expression of CerS2/Lass2, Histochem. Cell Biol. 129 (2) (2008) 233–241.
[48] D. Hartmann, J. Lucks, S. Fuchs, S. Schiffmann, Y. Schreiber, N. Ferreirós, et al., Long chain ceramides and very long chain ceramides have opposite effects on human breast and colon cancer cell growth, Int. J. Biochem. Cell Biol. 44 (4) (2012) 620–628.
[49] S.A. Saddoughi, B. Ogretmen, Diverse functions of ceramide in cancer cell death and proliferation, Adv. Cancer Res. 117 (2013) 37–58.
[50] Y. Matsuoka, A. Yamashita, M. Matsuda, K. Kawai, T. Sawa, F. Amaya, NLRP2 inflammasome in dorsal root ganglion as a novel molecular platform that produces inflammatory pain hypersensitivity, Pain 160 (9) (2019) 2149–2160.
[51] E.K. Joseph, J.D. Levine, Caspase signalling in neuropathic and inflammatory pain in the rat, Eur. J. Neurosci. 20 (11) (2004) 2896–2902.
[52] K. Nakajima, Y. Tohyama, S. Kohsaka, T. Kurihara, Ceramide activates microglia to enhance the production/secretion of brain-derived neurotrophic factor (BDNF) without induction of deleterious factors in vitro, J. Neurochem. 80 (4) (2002) 697–705.
[53] H. Scheiblich, A. Schlütter, D.T. Golenbock, E. Latz, P. Martinez-Martinez, M. T. Heneka, Activation of the NLRP3 inflammasome in microglia: the role of ceramide, J. Neurochem. 143 (5) (2017) 534–550.
[54] Y.H. Zhang, M.R. Vasko, G.D. Nicol, Ceramide, a putative second messenger for nerve growth factor, modulates the TTX-resistant Na(+) current and delayed rectifier K(+) current in rat sensory neurons, J. Physiol. 544 (2) (2002) 385–402.